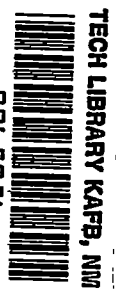


3628

NACA TN 2204

0065054



NATIONAL ADVISORY COMMITTEE FOR AERONAUTICS

TECHNICAL NOTE 2204

GUST-TUNNEL INVESTIGATION OF A WING MODEL WITH
SEMICHORD LINE SWEPT BACK 60°

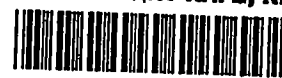
By Harold B. Pierce

Langley Aeronautical Laboratory
Langley Air Force Base, Va.



Washington
October 1950

AFWING
TECHNICAL NOTE 2204
OCT 1950



NATIONAL ADVISORY COMMITTEE FOR AERONAUTICS

TECHNICAL NOTE 2204

GUST-TUNNEL INVESTIGATION OF A WING MODEL WITH
SEMICHORD LINE SWEEP BACK 60°

By Harold B. Pierce

SUMMARY

An investigation was made in the Langley gust tunnel of a 60° sweptback-wing model to determine the effect of a large angle of sweep on gust loads. On the basis of the results, a simplified method of analysis, which uses a slope of the lift curve derived by the cosine law and which uses strip theory to estimate the penetration effect, appears to be applicable to the prediction of gust loads on wings swept as much as 60° . A summary curve representing the results of investigations with wing models having from 45° sweepforward to 60° sweepback is presented.

INTRODUCTION

A simplified method for predicting gust loads for airplanes having swept wings was presented in reference 1. Results calculated by this method were compared with experimental results for related wings having the semichord line swept back 45° (reference 1), swept back 30° (reference 2), and swept forward 45° (reference 3). In each case, the agreement between experiment and calculation showed the method to be adequate. The results also indicated that the maximum acceleration increment depends on the slope of the lift curve of an equivalent straight wing (reference 1) multiplied by the cosine of the angle of sweep and on the effect of the gradual penetration of the sweptback wing into the gust. Inasmuch as the method of reference 1 contains many simplifying assumptions, its applicability beyond the range of sweep angles tested (45°) was doubtful. Accordingly, the investigations in references 1 to 3 were extended to include gust-tunnel tests of a wing model having the semichord line swept back 60° and having an aspect ratio of 1.46. This paper presents the results of the gust-tunnel investigation of the 60° sweptback-wing model and compares these results with those from calculations made by the method of reference 1.

APPARATUS AND TESTS

A photograph of the model used in the tests is shown as figure 1 and the plan form of the model is shown in figure 2. The wing of the model was derived from that of the equivalent straight-wing model of reference 1 by rotating the straight wing about the semichord point at the plane of symmetry so that the constant-length semichord line moved back through an angle of 60° . The leading edge of the center section and the tips were modified to the dimensions shown in figure 2. In order to provide space for the batteries and the accelerometer in the wing of the model, the center section has smooth bulges projecting from the top and bottom surfaces. The thickness at the center section is therefore about double the thickness that the wing would have without the bulges. The characteristics of the model and the test conditions are given in table I. The slope of the lift curve determined by force tests included in the table was obtained from tests made in the Langley free-flight tunnel on the model with the tail off.

The center-of-gravity position shown in table I was calculated from the force tests to give the same static stability as that of the models previously tested (references 1 to 3). Because of a test limitation on the length of the model, the horizontal tail is in a position where it would be expected to contribute to the maximum value of the acceleration increment recorded in passage through a sharp-edge gust. In order to reduce the contribution, the horizontal-tail area was kept as small as practical. As a result, the tail volume (that is, tail area times tail length) of the present model is about 25 percent less than that of the previous models.

The gust tunnel and its equipment are described in references 1 and 4. The profile of the sharp-edge gust used in the tests is shown in figure 3 as the ratio of the local gust velocity to average maximum gust velocity as a function of the penetration in mean wing chords of the model.

Tests of the 60° sweptback-wing model consisted of 10 flights of the model through the gust profile shown in figure 3. Measurements of forward velocity, gust velocity, normal-acceleration increment, and pitch-angle increment were made during each flight.

PRECISION

The measured quantities are estimated to be accurate within the following limits for any single test or run:

Acceleration increment, Δn , g units	± 0.05
Forward velocity, feet per second	± 0.5
Gust velocity, feet per second	± 0.1
Pitch-angle increment, $\Delta \theta$, degrees	± 0.1

Results from repeat flights had a maximum dispersion of not more than $\pm 0.05g$. This dispersion is the result of small variations in the test conditions, the effect of which cannot be eliminated by corrections to the data.

RESULTS

The records for all flights were evaluated to obtain histories of the normal-acceleration increment and pitch-angle increment during the traverse of the gust. Representative test results are shown in figure 4. The acceleration increment Δn and the pitch-angle increment $\Delta \theta$ are plotted against the distance of the airplane center of gravity from the leading edge of the gust-tunnel test section measured in mean chords.

The maximum acceleration increment for each test flight was determined from the flight record and was corrected to a weight of 9.25 pounds, a forward velocity of 60 miles per hour, and a gust velocity of 10 feet per second on the basis of the assumption that the increment is inversely proportional to the weight and directly proportional to forward speed and gust velocity. This correction was made so that these results can be compared with those of references 1 to 3 and so that the effect of small variations in launching speed and gust velocity can be eliminated. The average of the corrected maximum acceleration increments was 1.22.

Figure 4 shows that the model has appreciable pitching motion at the point of maximum acceleration. In order that a comparison of the experimental values with the values calculated according to the method of reference 1 can be made, the effect of pitching motion was removed from the experimental data. This adjustment was made by the approximate method of equation (3) of reference 1, and the resultant value of maximum acceleration increment is 1.18.

CALCULATIONS

Calculations to predict the response of the model to the test gust were made according to the method set forth in reference 1. As in reference 1, the unsteady-lift function C_{L_g} for penetration of a sharp-edge gust and the function C_{L_α} for a sudden change of angle of attack are in the form of ratios of the lift coefficient at any distance to the lift coefficient after an infinite distance has been traversed. The functions were obtained from the curves of reference 5 for infinite aspect ratio, and the function C_{L_g} was modified by strip theory to take into account the gradual penetration of the 60° sweptback wing into the gust. The curve for C_{L_α} and the modified curve for C_{L_g} are shown in figure 5 in terms of mean chords of the test model. For comparison the unmodified curve for C_{L_g} is also shown in figure 5. Two slopes of the lift curve were used: One was that of the straight-wing model of reference 1 multiplied by the cosine of the angle of sweep; the other was the slope determined from force tests made under steady-flow conditions with the tail of the model off. The maximum acceleration increment Δn determined by use of the cosine-law slope was 1.00 and that determined by use of the steady-flow slope was 0.89.

DISCUSSION

The maximum experimental acceleration increment reduced to zero pitch is compared with the calculated results in the following table:

Experimental Δn_{\max} reduced to zero pitch (g units)	Calculated Δn_{\max} (reference 1) (g units)	
	Cosine-law slope	Steady-flow slope
1.18	1.00	0.89

The comparison of experimental and calculated results in the foregoing table shows that the value calculated by use of the cosine-law slope of the lift curve is about 0.2g lower than that obtained by experiment. The value calculated by substitution of the measured steady-flow slope of the lift curve for the cosine-law slope is about 0.3g lower than

experiment. Although the use of the cosine-law slope indicates better agreement with experiment than the measured slope, the agreement is not considered adequate to verify the use of the cosine-law slope of the lift curve. The configuration, however, was such that a discrepancy would be expected to exist between experiment and a calculation that considers the effect of the gust on the wing only. For instance, at the time of maximum acceleration increment in the sharp-edge gust, the tail surface of this model has penetrated the gust about 3 chords so that an appreciable contribution to the recorded acceleration increment might be expected.

In order to determine whether the contribution of the tail surface caused the discrepancy observed, an estimate was made of the contribution of the tail surface to the recorded acceleration increment. Rough calculations made by use of the experimental acceleration-increment and pitch-angle-increment data indicated that the effect of pitching and vertical motions on the tail load cancel and leave only the effect of the gust and the wing downwash to be considered. Accordingly, the acceleration increment due to the tail in the sharp-edge gust was estimated from the following equation

$$\Delta a_t = \frac{\rho m_t U V S_t}{2W} \left(1 - \frac{d\varepsilon}{d\alpha} \right) \left[C_{L_g}(s_t) \right]_{s_{t1}}$$

where the slope of the lift curve of the tail m_t , was taken as 4.05 and the downwash factor $d\varepsilon/d\alpha$ was estimated from the force tests as being about 0.5. The build up of lift on the horizontal tail $C_{L_g}(s_t)$ is a function of the penetration of the surface into the gust in terms of mean chords of the tail s_t and is assumed to be the same as the unmodified curve for C_{L_g} in figure 5. The value of $C_{L_g}(s_t)$ at the number of chords of penetration into the gust desired, s_{t1} , is represented by the term $\left[C_{L_g}(s_t) \right]_{s_{t1}}$. At the time of the maximum recorded acceleration increment, the tail has penetrated the gust about 3 chords and the value of $\left[C_{L_g}(s_t) \right]_{s_{t1}}$ is about 0.78. Substitution of these

values together with others from table I in the preceding equation indicated that the tail could contribute about 0.13g to the total response. This estimated contribution of the horizontal tail accounts for the greatest part of the discrepancy between the experimental results and those calculated by use of the cosine-law slope of the lift curve. On the basis of the foregoing analysis, the simplified method of calculation given in reference 1, which uses a slope of the lift curve derived by

the cosine law and strip theory to estimate the penetration effect, appears to be applicable to the prediction of gust loads on wings swept as much as 60° .

Figure 6 compares the results of the present investigation with those of references 1 to 3. The load ratios given are the ratios of the acceleration increments at the angle of sweep to the corresponding (experimental or calculated) acceleration increments at zero angle of sweep. Examination of figure 6 shows that the load from penetration of a given gust decreases rapidly as the wing is swept either forward or backward. The load for the 60° sweptback wing is about one-half that of the equivalent straight wing.

CONCLUDING REMARKS

On the basis of the analysis made, the gust load on a model with a wing having the semichord line swept back 60° appears to be dependent on the effect of the gradual penetration of the gust on the unsteady-lift function and on a slope of the lift curve at least as great as that of the equivalent straight wing multiplied by the cosine of the angle of sweep. A summary curve representing the results of the investigation of models having wings with angles of sweep ranging from -45° to the present 60° shows that the load in a given gust decreases rapidly as the wing is swept either backward or forward.

Langley Aeronautical Laboratory
National Advisory Committee for Aeronautics
Langley Air Force Base, Va., August 4, 1950

REFERENCES

1. Pierce, Harold B.: Tests of a 45° Sweptback-Wing Model in the Langley Gust Tunnel. NACA TN 1528, 1948.
2. Reisert, Thomas D.: Gust-Tunnel Investigation of a Wing Model with Semichord Line Swept Back 30° . NACA TN 1794, 1949.
3. Pierce, Harold B.: Gust-Tunnel Investigation of a 45° Sweptforward-Wing Model. NACA TN 1717, 1948.
4. Donely, Philip: An Experimental Investigation of the Normal Acceleration of an Airplane Model in a Gust. NACA TN 706, 1939.
5. Jones, Robert T.: The Unsteady Lift of a Wing of Finite Aspect Ratio. NACA Rep. 681, 1940.

TABLE I

CHARACTERISTICS OF MODEL AND TEST CONDITIONS

Weight, W, pounds	9.63
Wing area, S, square feet	6.17
Wing loading, W/S, pounds per square foot	1.56
Wing span, b, feet	3.0
Wing aspect ratio, b^2/S	1.46
Wing chords measured parallel to plane of symmetry:	
Mean geometric chord, feet	2.06
Root chord, c_s , feet	2.29
Tip chord, c_t , feet	1.412
Sweep angle of wing semichord line, degrees	60
Slope of wing lift curve determined by force tests, per radian	1.95
Slope of wing lift curve determined by multiplying lift- curve slope of equivalent straight wing (reference 1) by cosine of sweep angle, per radian	2.205
Center-of-gravity position, percent wing mean geometric chord	31
Horizontal tail area, S_t , square foot	0.73
Tail mean geometric chord, foot	0.42
Gust velocity, U, feet per second	10
Forward velocity, V, miles per hour	60
Mass density of air, ρ , slug per cubic foot	0.00238



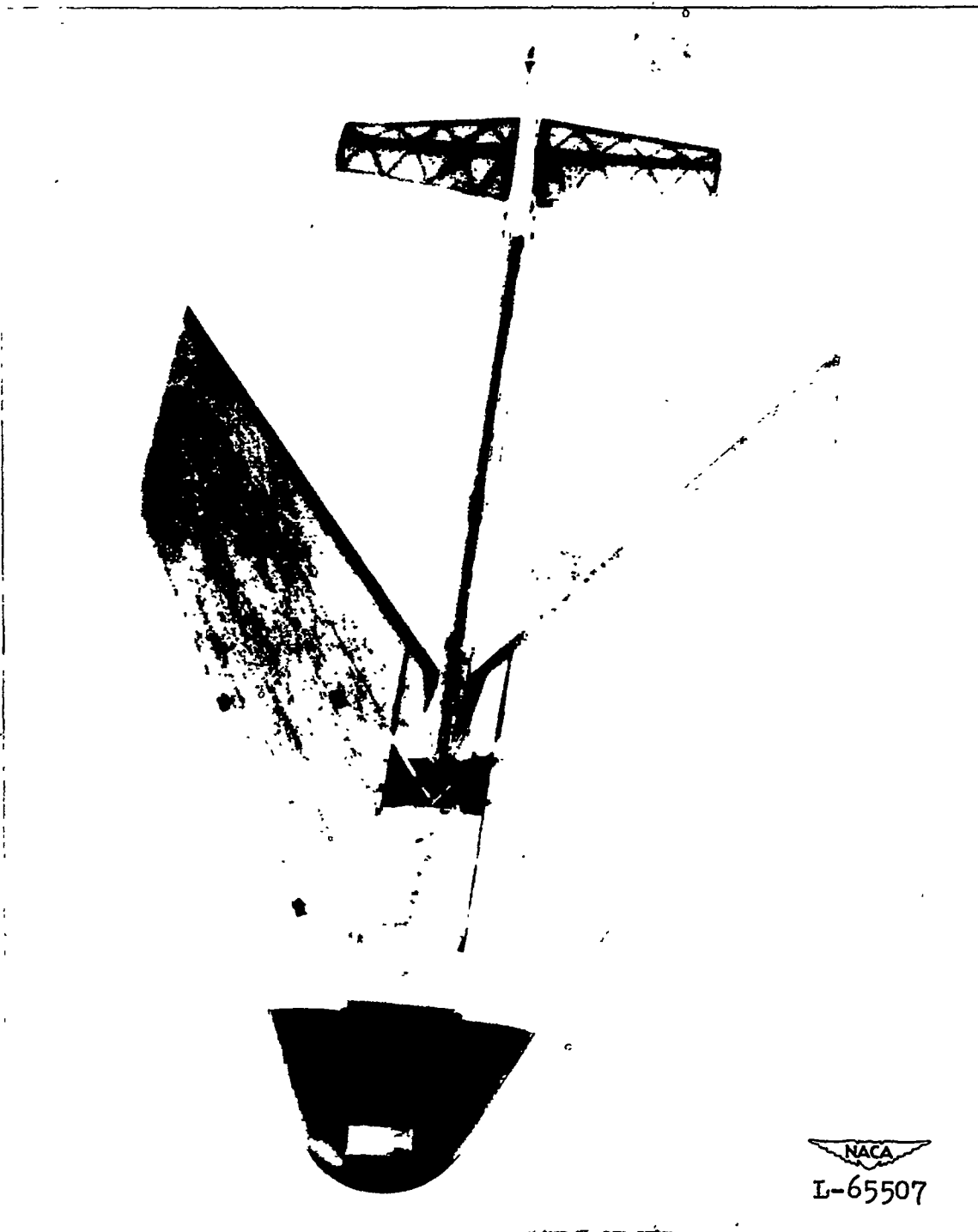


Figure 1.- Model with semichord line of wing swept back 60° .



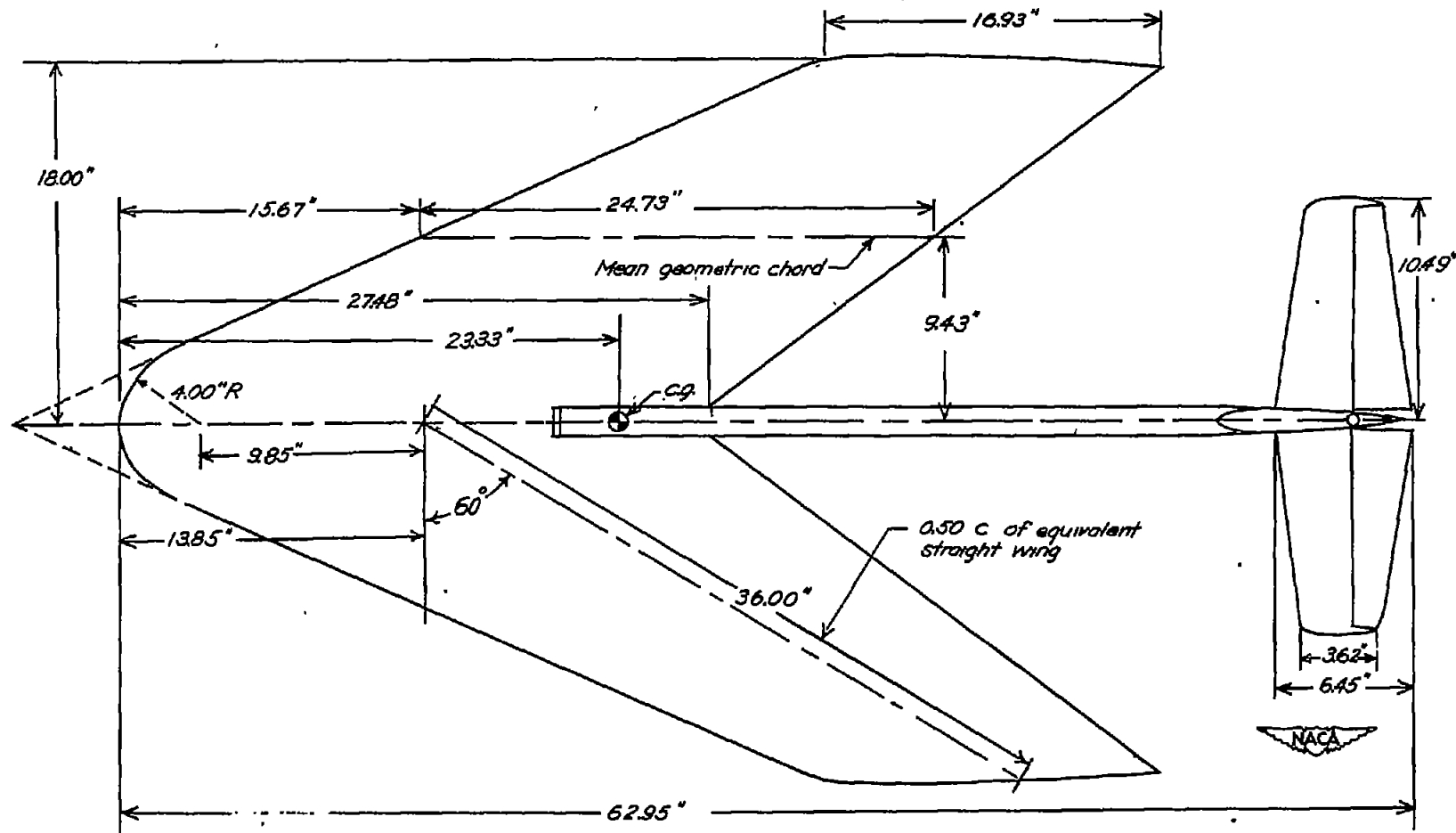


Figure 2.- Plan form of model with 60° sweptback wing.

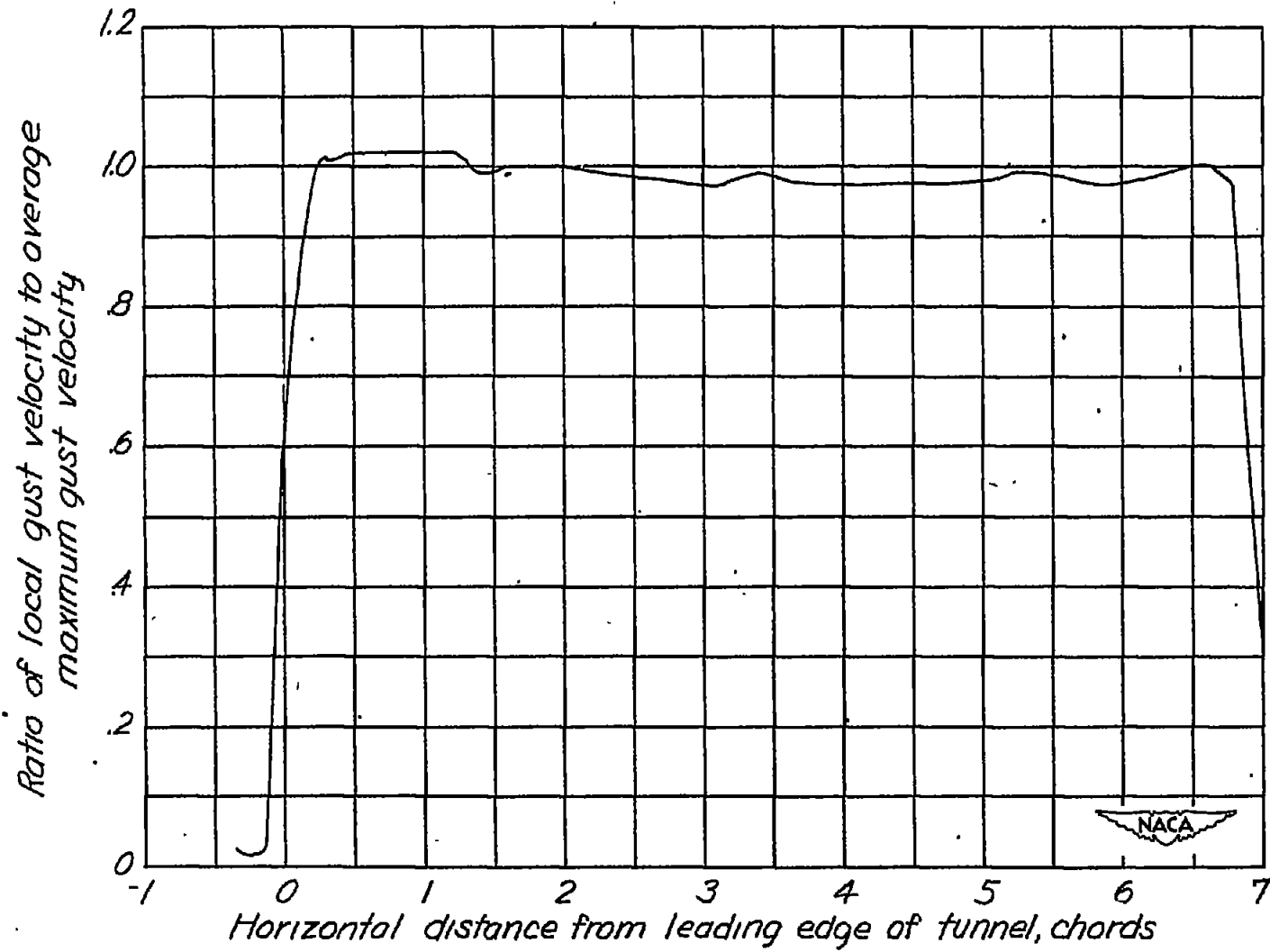


Figure 3.- Velocity distribution through gust-tunnel jet. Sharp-edge gust.

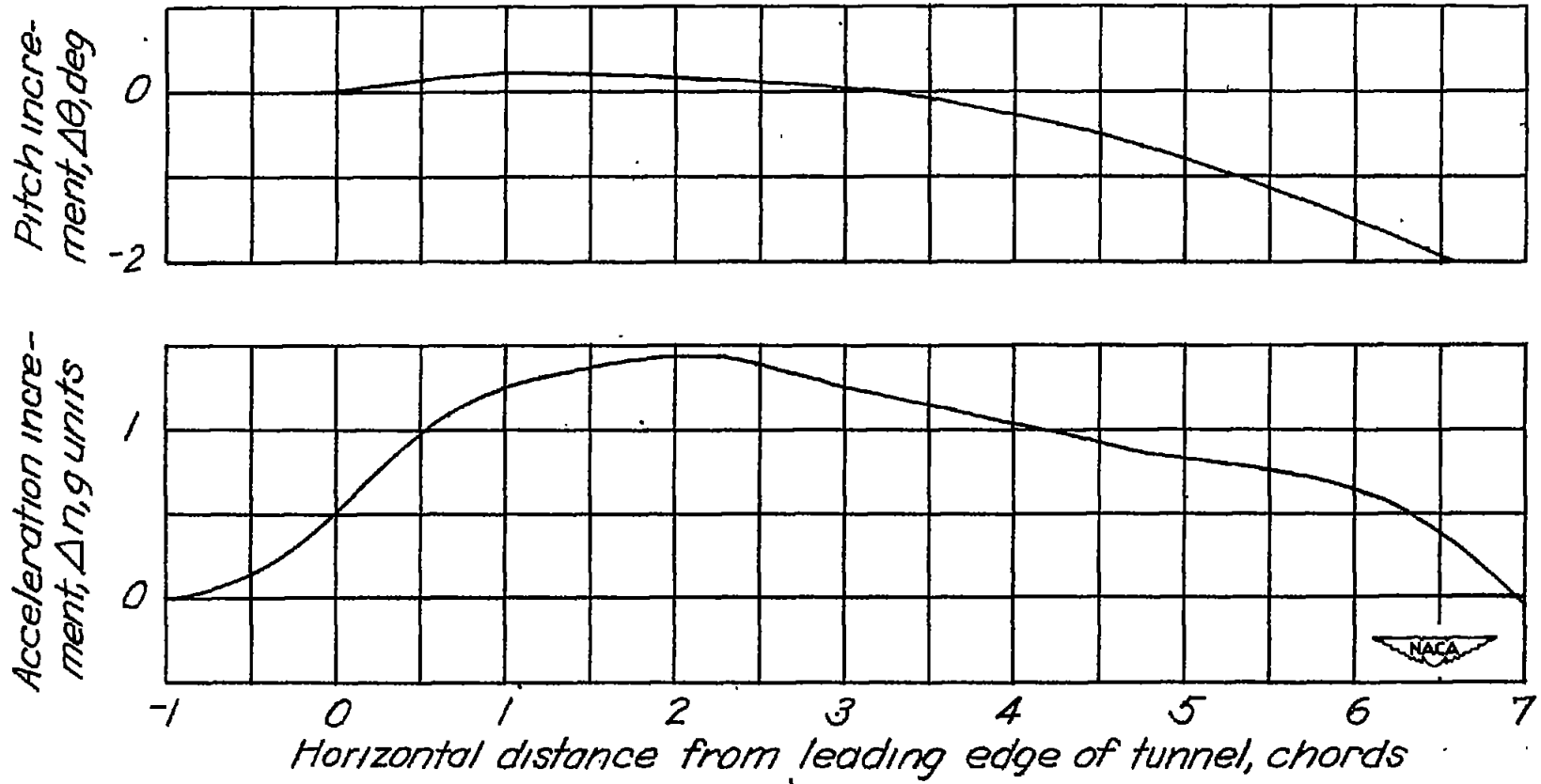


Figure 4.- Representative history of events in sharp-edge gust.

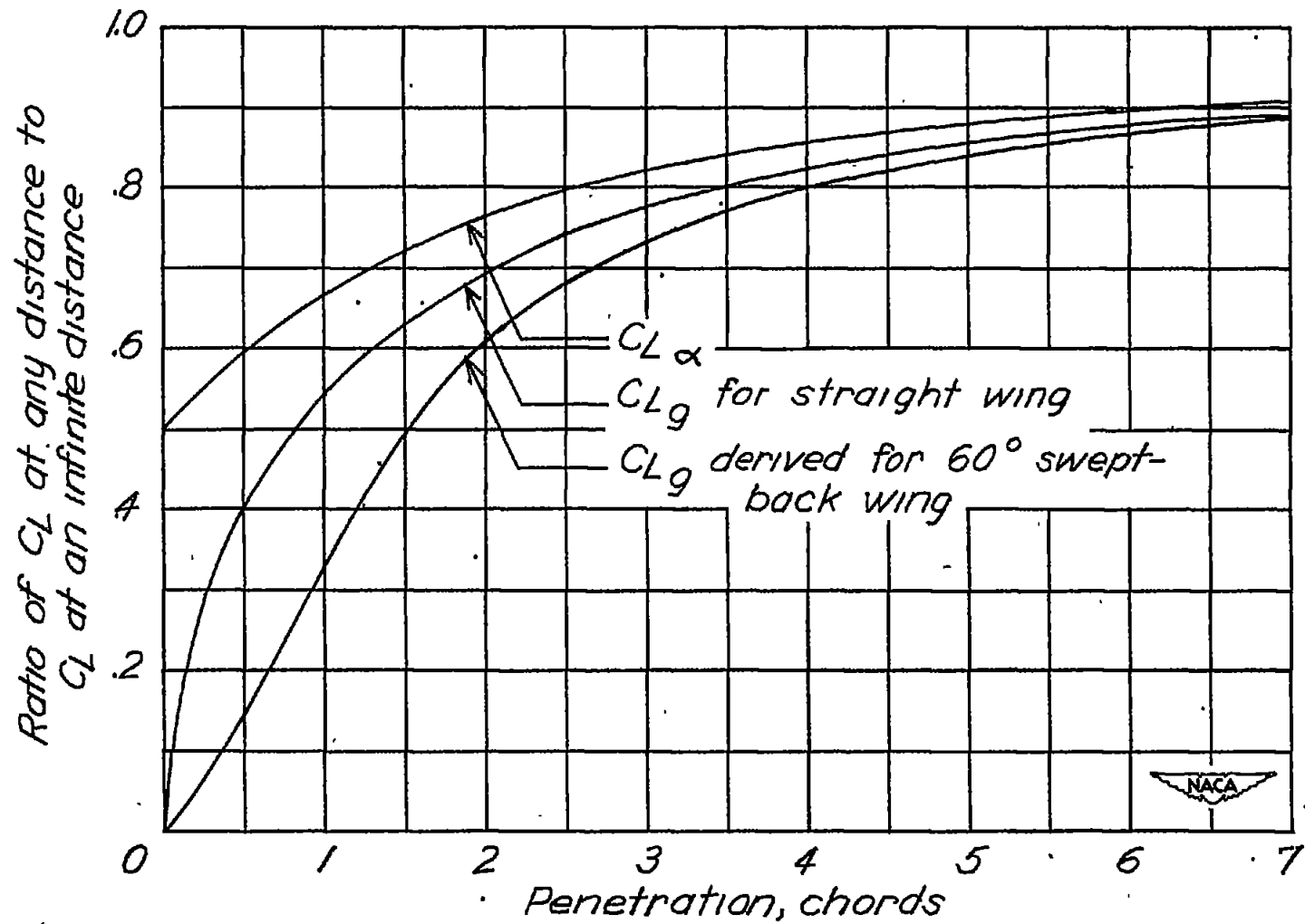


Figure 5.- Curves of C_{Lg} and $C_{L\alpha}$ based on unsteady-lift functions for infinite aspect ratio.

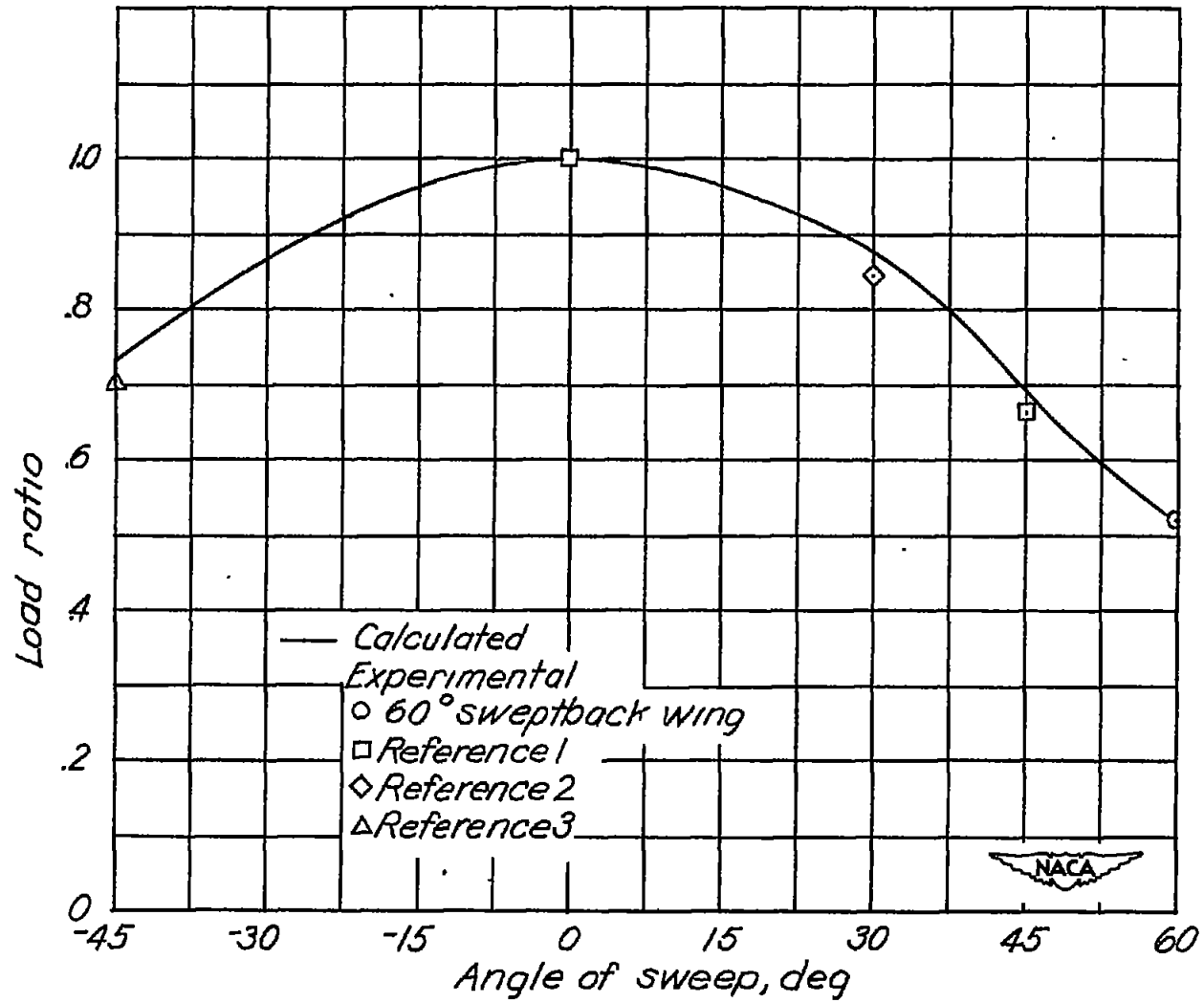


Figure 6.- Effect of sweep on gust load. Sharp-edge gust.